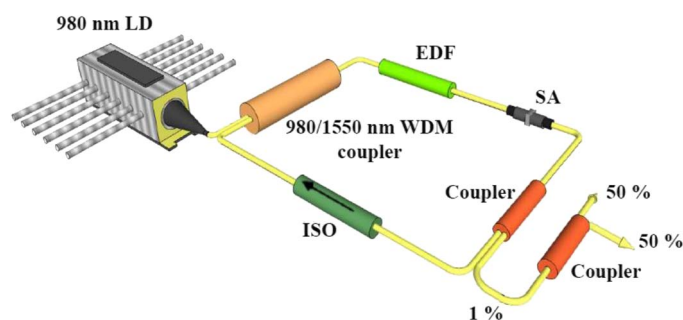


# C-Band Q-Switched Fiber Laser Using Titanium Dioxide (TiO<sub>2</sub>) As Saturable Absorber

Volume 8, Number 1, February 2016

H. Ahmad  
S. A. Reduan  
Zainal Abidin Ali  
M. A. Ismail  
N. E. Ruslan  
C. S. J. Lee  
R. Puteh  
S. W. Harun



DOI: 10.1109/JPHOT.2015.2506169  
1943-0655 © 2015 IEEE

# C-Band Q-Switched Fiber Laser Using Titanium Dioxide (TiO<sub>2</sub>) As Saturable Absorber

H. Ahmad,<sup>1</sup> S. A. Reduan,<sup>1</sup> Zainal Abidin Ali,<sup>2</sup> M. A. Ismail,<sup>1</sup> N. E. Ruslan,<sup>1</sup>  
C. S. J. Lee,<sup>1</sup> R. Puteh,<sup>2</sup> and S. W. Harun<sup>3</sup>

<sup>1</sup>Photonics Research Centre, University of Malaya, 50603 Kuala Lumpur, Malaysia

<sup>2</sup>Department of Physics, Faculty of Science, University of Malaya, 50603 Kuala Lumpur, Malaysia

<sup>3</sup>Department of Electrical Engineering, Faculty of Engineering,  
University of Malaya, 50603 Kuala Lumpur, Malaysia

DOI: 10.1109/JPHOT.2015.2506169

1943-0655 © 2015 IEEE. Translations and content mining are permitted for academic research only.

Personal use is also permitted, but republication/redistribution requires IEEE permission.

See [http://www.ieee.org/publications\\_standards/publications/rights/index.html](http://www.ieee.org/publications_standards/publications/rights/index.html) for more information.

Manuscript received October 18, 2015; revised November 22, 2015; accepted December 2, 2015. Date of publication December 7, 2015; date of current version December 22, 2015. This work was supported in part by the University of Malaya and in part by the Malaysian Ministry of Higher Education under Grant LRGS(2015)/NGOD/UM/KPT, Grant UM.C/625/1/HIR/MOHE/SCI/29, Grant RU007/2015, and Grant PG009-2014A. Corresponding author: H. Ahmad (e-mail: harith@um.edu.my).

**Abstract:** We demonstrate a passively Q-switched erbium fiber laser using titanium dioxide (TiO<sub>2</sub>) as a saturable absorber. The TiO<sub>2</sub> saturable absorber was fabricated as a polymer composite film and sandwiched between fiber ferrules. Q-switched pulsing starts with the assistance of physical disturbance of the laser cavity (by lightly tapping the cavity to induce instability) at 140 mW and lasts until 240 mW. The repetition rate increases with the pump power from 80.28 to 120.48 kHz. On the other hand, the pulsewidth decreases from 2.054  $\mu$ s until it reaches a plateau at 1.84  $\mu$ s. The Q-switched fiber laser exhibits two competing modes: at 1558.1 and 1558.9 nm as the pump power increases. A high signal-to-noise ratio of 49.65 dB is obtained.

**Index Terms:** Q-switched, TiO<sub>2</sub>.

## 1. Introduction

Q-switching is a common technique in that is used to produced a pulsed laser output [1]. Q-switching is obtained by modulating the quality factor Q of laser cavity such that a series of short, intense pulses produced, with a higher Q factor resulting in lower losses per oscillation cycle. Thus, the Q factor acts as ratio of energy stored in the active medium to energy lost per oscillation cycle [2]–[4]. The repetition rate of Q-switched lasers is usually in the kHz region, as compared to the repetition rate of mode locked pulse lasers that are typically in the MHz range. Furthermore, the pulsewidth of the Q-switched laser fall within a range of ms to few tens of ns [4]. As a result of this, there has now been a great interest in Q-switched laser because of the advantages of long pulsed lasers in many important applications such as material processing, medicine, environmental sensing, and nonlinear experiments [5]–[7].

There are two ways to generate Q-switched pulse: active (exploiting, e.g., electro-optic modulator) or passive (using, e.g., saturable absorber) Q-switching. However, passive Q-switching is a more useful and cost-effective way to produce pulsed laser than active Q-switching, which requires additional switching electronics [4]. There are growing interest in Q-switched fiber lasers

because of their advantages, including high efficiency, flexibility, compactness, and high spatial beam quality [1]. Furthermore, fiber lasers have significant advantages over their bulk optic counterparts in terms of their small footprint, robust beam confinement and environmental stability, all of which are highly desirable traits for real world applications.

The discovery of graphene by Novoselov *et al.* [8], has started a “gold rush” towards understanding and exploiting 2-D materials. More and more 2-D materials are being studied in the quest to find the successor to graphene. It was discovered that 2-D materials reveal different electronic, optical, thermal and mechanical properties from its 3-D form [8]. In the field of optoelectronics, they can be used for photovoltaics, photodetection and photoluminescence. The existence of Pauli blocking property inside these materials enables them to be utilized as saturable absorbers to generate Q-switched and mode-locked lasers. Indeed, 2-D materials such as transition metal dichalcogenides (TMDs) [9]–[11], which has 60 different variations, has been utilized as saturable absorber to generate passive Q-switched and mode-locked fiber lasers [12]–[17]. Topological insulators such as  $\text{Bi}_2\text{Te}_3$  and  $\text{Sb}_2\text{Te}_3$  [18], [19], which are a class of materials that only permits the flow of electrons on its surface, have also been successfully demonstrated to achieve Q-switched and mode-locked fiber lasers [20]–[23].

An ideal saturable absorber has a broadband absorption, ultrafast recovery time ( $\sim\text{ps}$ ), low saturation intensity, appropriate modulation depth, high damage threshold as well as cost- and time-efficient to make. Titanium dioxide ( $\text{TiO}_2$ ) has a recovery time of  $\sim 1.5$  ps when observed using 780 nm, 250-fs laser [24]. Furthermore, an open-aperture Z-scan on  $\text{TiO}_2$  films reveals nonlinear optical properties known as saturable absorption and two-photon absorption [25]–[28]. Although the band gap of  $\text{TiO}_2$  is  $\sim 3.2$  eV (387 nm) [29]–[31], spectral absorption by  $\text{TiO}_2$  can extend until the near-infrared (NIR) region [32]. This can be explained by the quantum size effect of  $\text{TiO}_2$ , where the absorption depends on the crystal form and particle size [33].

In this paper, we introduce  $\text{TiO}_2$  as saturable absorber (SA) to generate passive Q-switched fiber laser operating in C-band. Despite having a band gap in the UV region, by using white light source (WLS), we have discovered that the  $\text{TiO}_2$  SA absorbs at near infrared region (NIR). When pump power is increased, the repetition rate and pulse width observed are as expected from a Q-switched laser.

## 2. Saturable Absorber Q-Switcher

### 2.1. Saturable Absorber Preparation

In this experiment,  $\text{TiO}_2$  nanostructures used was obtained from Sigma Aldrich (Malaysia) Sdn. Bhd. and used without further purification. Fig. 1 shows the field emission scanning electron microscopy (FESEM) image, Uv-Vis spectrum and the X-ray diffractions (XRD) pattern of the  $\text{TiO}_2$ . The sizes of the nanostructures were in the range of 20–50 nm. The  $\text{TiO}_2$  exhibits a strong absorption band at around 354 nm. The  $\text{TiO}_2$  provided was of the anatase group. The performance of  $\text{TiO}_2$  as a saturable absorber was tested by embedding it into a polymer based thin film. The thin film was developed by heating 1-gram of agar in a 50 ml of deionized water for 15 minutes at  $300^\circ\text{C}$  before 0.05 g of  $\text{TiO}_2$  was added. The mixture was continuously stirred before being poured into a 25-ml mold. The mixture was left to dry in  $27^\circ\text{C}$  environment for 3 days. The thickness of the thin film was measured to be  $0.15 \pm 0.01$  mm. Fig. 1(c) XRD pattern of the  $\text{TiO}_2$  (from Sigma Web).

### 2.2. Nonlinear Optical Absorption Characteristics of Titanium Dioxide, $\text{TiO}_2$ Sample

Twin detector technique was used to characterize the nonlinear optical response of saturable absorber titanium dioxide,  $\text{TiO}_2$ . The illumination source is a passively mode-locked fiber laser with a repetition rate of 26 MHz, pulse width of 600 fs and 1560 nm central wavelength ( $\lambda_c$ ). The output powers from both detectors were recorded as we gradually decreased the attenuation value.

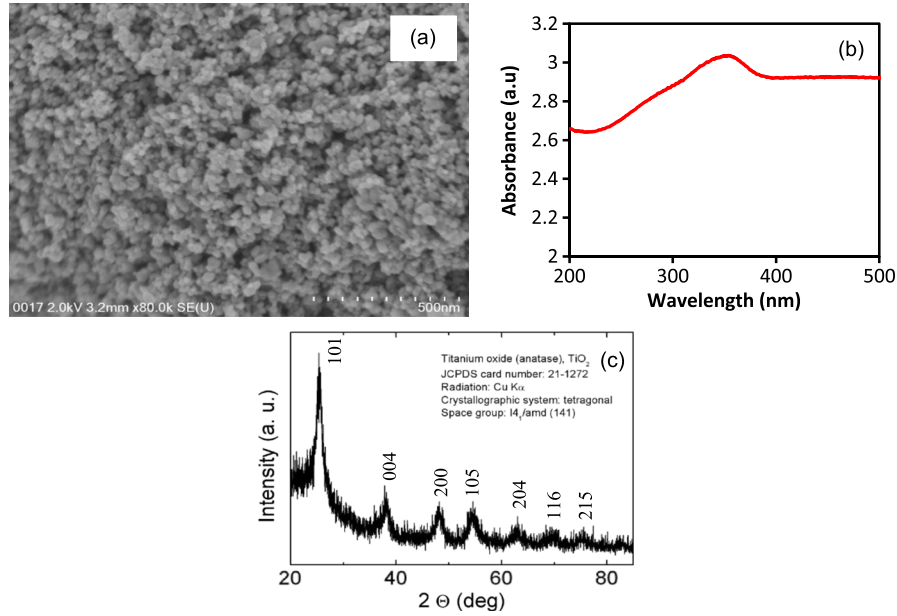


Fig. 1. (a) FESEM image and (b) Uv-vis absorbance of the TiO<sub>2</sub> nanostructures (c) XRD pattern of TiO<sub>2</sub> (from Sigma Web).

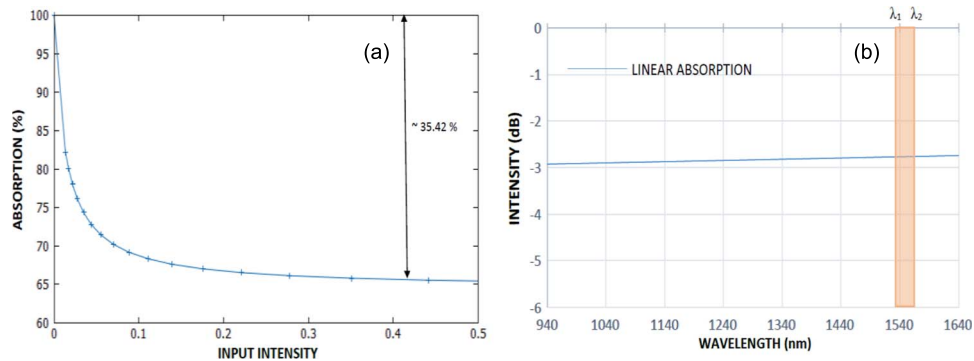


Fig. 2. (a) Measured saturable absorption data. (b) Linear absorption of Titanium Dioxide, TiO<sub>2</sub> film (region in orange indicates C-band).

From the result, the absorption was calculated and later, was fitted using the following saturation model formula [34]:

$$\alpha(I) = \frac{\alpha_s}{1 + \frac{I}{I_s}} + \alpha_{ns} \quad (1)$$

where  $\alpha(I)$  is the absorption rate,  $\alpha_s$  is the saturable absorption,  $\alpha_{ns}$  is the unsaturable absorption,  $I$  is input intensity, and  $I_{sat}$  is saturation intensity.

The absorptions at various input intensities were recorded and plotted as shown in Fig. 2(a) after fitting using saturation model formula (1). The saturation intensity and modulation depth of the saturable absorber were determined to be 0.013 MW/cm<sup>2</sup> and 35.41%, respectively. The saturation intensity for different saturable absorber are 58.59 MW/cm<sup>2</sup> for Bi<sub>2</sub>Te<sub>3</sub> [35] and 0.43 MW/cm<sup>2</sup> for MoS<sub>2</sub> [36]. Fig. 2(b) shows the linear absorption of the titanium dioxide film. It shows that the intensity of white light source decreases slightly with the presence of titanium dioxide, TiO<sub>2</sub> film. This proves that the TiO<sub>2</sub> SA can absorb in the near-infrared region. The range between λ<sub>1</sub> to λ<sub>2</sub> in Fig. 2(b) indicates the region of C-band.

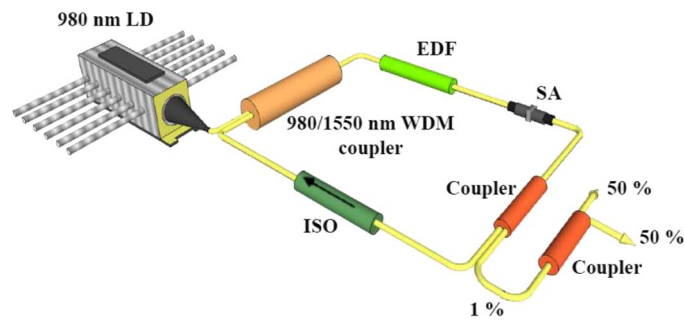


Fig. 3. Schematic of Q-switched fiber laser: WDM (wavelength division multiplexer), EDF (erbium-doped fiber), ISO (isolator), SMF (single mode fiber), and SA (saturable absorber).

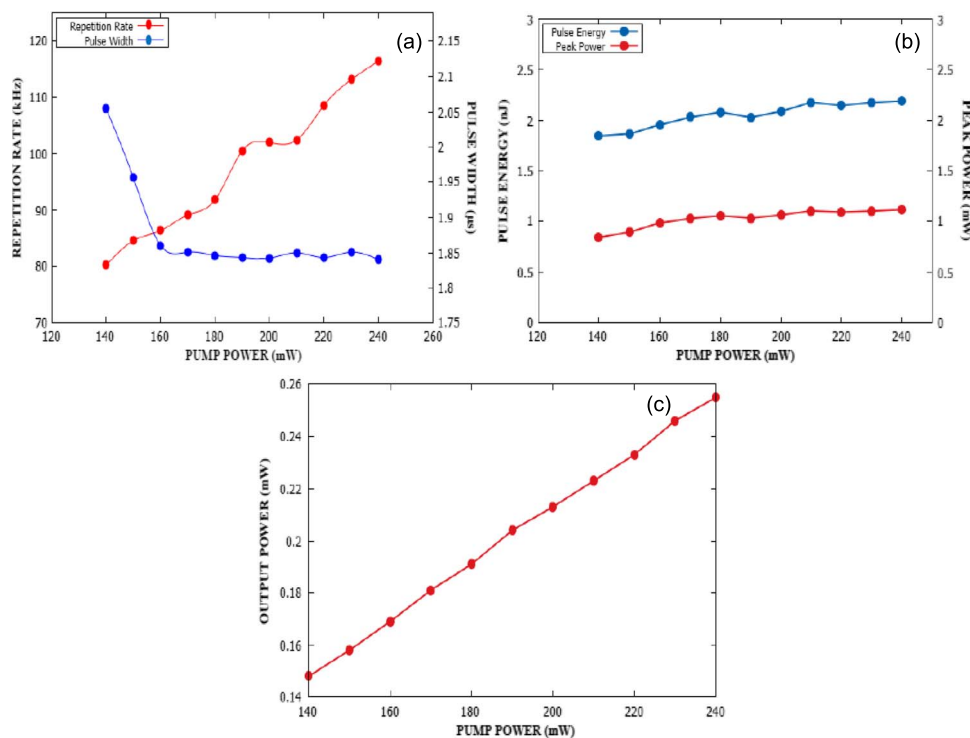


Fig. 4. Trends for (a) repetition rate and pulse width (b) pulse energy and peak power (c) output power as a function of input pump power.

### 2.3. Q-Switched Fiber Laser Setup

Schematic diagram of fiber laser setup is shown in Fig. 3. Three-meter-long Erbium-doped fiber (EDF) (IsoGain I-25(980/125), Fibercore; cut-off wavelength, 900–970; numerical aperture, 0.23–0.26; absorption 35–45 @ 1550 nm) was used as gain medium and pumped by a 974 nm LD, coupled via 980/1550-nm fused wavelength division multiplexer (WDM). An isolator (ISO) was used to preserve the unidirectional light operation. A 99/1 fiber coupler was spliced into the cavity after the SA. The 1% output port is further divided by 50/50 fiber coupler to enable two simultaneous measurements. Standard single mode fiber (SMF-28) was used for the rest of the fibers. A 500-MHz oscilloscope (YOKOGAWA DLM2054) combined with a 1.2-GHz photo-detector; a radio frequency spectrum analyzer, optical power meter and an optical spectrum analyzer (YOKOGAWA AQ6370C) were used simultaneously to monitor the spectrum, radio-frequency (RF) spectrum, output power, and time profile of the output pulse train, respectively.

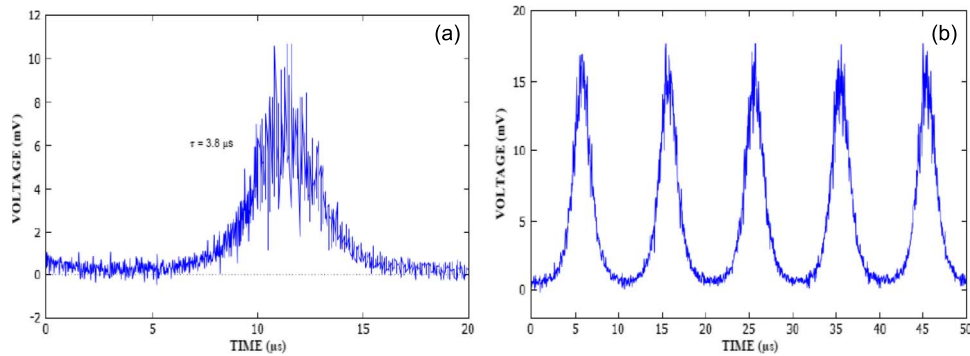


Fig. 5. Q-switched (a) pulse profile and (b) pulse train.

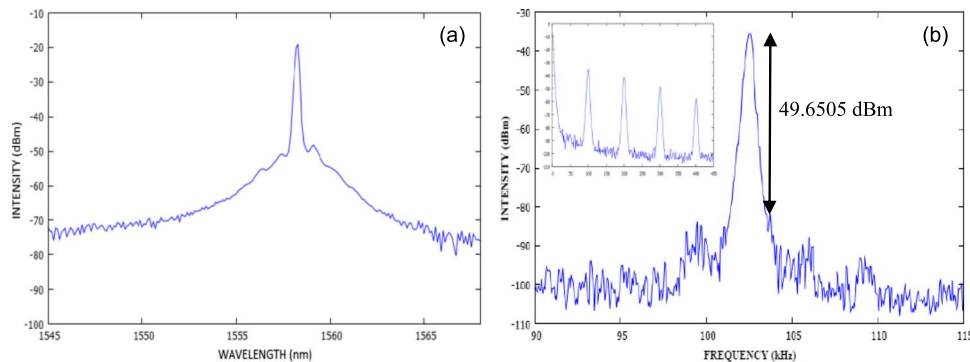


Fig. 6. Q-switched pulse emitted. (a) Output spectrum. (b) Radio-frequency optical spectrum and the wideband RF spectrum (insert).

### 3. Results and Discussion

Continuous wave laser operation started at pump power of 60 mW; when pump power reached  $\sim 140$  mW, Q-switching operation occurred. The initial pulse repetition rate is  $\sim 80.28$  kHz, with an output power of 0.148 mW. This corresponds to pulse energy of  $\sim 1.844$  nJ and peak power of 0.843 mW. The operation shows a typical signature for Q-switching operation where the repetition rate is pump-dependent up to  $\sim 240$  mW as shown in Fig. 4(a) [4]. Pulsing phenomena was not observed before the addition of  $\text{TiO}_2$  inside our laser cavity. Therefore, we conclude that; it is the  $\text{TiO}_2$  that is responsible for inducing Q-switching pulse in our cavity. When the pump power was increased, the repetition rate increased while the pulse width decreased, consistent with results obtained by other Q-switched lasers [6], [37], [38]. Fig. 4(b) illustrates the trends of pulse energy and peak power as a function of input pump power, and it can be seen that for both scenarios the pulse energy and peak power increases as the pump power increases. The output power also increases gradually as the pump power increases, as shown in Fig. 4(c).

Fig. 5(a) shows a pulse profile, having a FWHM  $\sim 3.8 \mu\text{s}$ , comparable with other SAs of Q-switched fiber laser (e.g., gold nanocrystals [37]). The single-pulse profile shows microstructures that exist along the edge of the pulse, particularly at the peak due to mode beating phenomenon. Fig. 5(b) plots the pulse train for laser output at 210 mW pump power.

One peak is observed at the wavelength of 1558.9 nm as shown in Fig. 6(a). From Fig. 6(b), the signal-to-noise ratio of Q-switched fiber laser is over 49.6505, indicating that the Q-switched pulse is in a relatively stable regime. Apart from the fundamental and harmonic frequency peaks, there is no other frequency component in the RF spectrum with wider span signifying that the Q-switched pulse produced is stable.  $\text{TiO}_2$  based SAs are capable of generating pulses with narrower repetition rates that those generated by  $\text{MoS}_2$  based SAs [13], [14], which are



typically in the range of 10.6 to 173.1 kHz, but a wider range than MoSe<sub>2</sub> and black phosphorus based SAs, which typically range from 26.5 to 35.4 kHz and 6.98 to 15.78 kHz, respectively [39], [40].

#### 4. Conclusion

We demonstrate a passively Q-switched erbium-doped fiber laser using a TiO<sub>2</sub> based saturable absorber. The saturable absorber absorbs at the C-band, has modulation depth of 26.57%, and has saturation intensity of 0.21 MW/cm<sup>2</sup>. The repetition rate increases from 80.28 kHz to 120.48 kHz, and pulse width decreases from 2.054  $\mu$ s to 1.84  $\mu$ s as the pump power increases from 140 mW to 240 mW. The experimental results verified that the TiO<sub>2</sub> could be used as an effective saturable absorber to generate passive Q-switched fiber laser.

#### References

- [1] T.-Y. Tsai and Y.-C. Fang, "A saturable absorber Q-switched all-fiber ring laser," *Opt. Exp.*, vol. 17, no. 3, pp. 1429–1434, 2009.
- [2] A. Kurkov, "Q-switched all-fiber lasers with saturable absorbers," *Laser Phys. Lett.*, vol. 8, no. 5, p. 335, 2011.
- [3] P. Morkel, K. Jedrzejewski, E. Taylor, and D. Payne, "Short-pulse, high-power Q-switched fiber laser," *IEEE Photon. Technol. Lett.*, vol. 4, no. 6, pp. 545–547, Jun. 1992.
- [4] O. Svelto and D. C. Hanna, *Principles of Lasers*. New York, NY, USA: Springer-Verlag, 2010.
- [5] R. Paschotta *et al.*, "Passively Q-switched 0.1-mJ fiber laser system at 1.53  $\mu$ m," *Opt. Lett.*, vol. 24, no. 6, pp. 388–390, 1999.
- [6] D. Popa *et al.*, "Graphene Q-switched, tunable fiber laser," *Appl. Phys. Lett.*, vol. 98, 2011, Art. ID 073106.
- [7] M. Siniaeva *et al.*, "Laser ablation of dental materials using a microsecond Nd: YAG laser," *Laser Phys.*, vol. 19, no. 5, pp. 1056–1060, May 2009.
- [8] K. S. Novoselov *et al.*, "Electric field effect in atomically thin carbon films," *Science*, vol. 306, no. 5696, pp. 666–669, Oct. 2004.
- [9] R. Lieth and J. Terhell, *Transition Metal Dichalcogenides Preparation and Crystal Growth of Materials With Layered Structures*. Berlin, Germany: Springer-Verlag, 1977, pp. 141–223.
- [10] K. H. Wang, K. Kalantar-Zadeh, A. Kis, J. N. Coleman, and M. S. Strano, "Electronics and optoelectronics of two-dimensional transition metal dichalcogenides," *Nature Nanotechnol.*, vol. 7, no. 11, pp. 699–712, 2012.
- [11] J. Wilson and A. Yoffe, "The transition metal dichalcogenides discussion and interpretation of the observed optical, electrical and structural properties," *Adv. Phys.*, vol. 18, no. 73, pp. 193–335, 1969.
- [12] Y. Huang and Z. Luo, "Passively Q-switched linear-cavity erbium-doped fiber laser with few-layer Ti: Bi<sub>2</sub>Se<sub>3</sub> saturable absorber," presented at the Fiber-Based Technol. Applications Conf., Wuhan, China, 2014.
- [13] H. Li *et al.*, "Passively-switched erbium-doped fiber laser based on few-layer MoS<sub>2</sub> saturable absorber," *IEEE Photon. Technol. Lett.*, vol. 27, no. 1, pp. 69–72, Jan. 2015.
- [14] Z. Luo *et al.*, "1-, 1.5-, and 2- $\mu$ m fiber lasers Q-switched by a broadband few-layer MoS<sub>2</sub> saturable absorber," *J. Lightw. Technol.*, vol. 32, no. 24, pp. 4077–4084, 2014.
- [15] S. Wang *et al.*, "Broadband few-layer MoS<sub>2</sub> saturable absorbers," *Adv. Mater.*, vol. 26, no. 21, pp. 3538–3544, 2014.
- [16] H. Zhang *et al.*, "Molybdenum disulfide (MoS<sub>2</sub>) as a broadband saturable absorber for ultra-fast photonics," *Opt. Exp.*, vol. 22, no. 6, pp. 7249–7260, 2014.
- [17] M. Zhang *et al.*, "Solution processed MoS<sub>2</sub>-PVA composite for sub-bandgap mode-locking of a wideband tunable ultrafast Er: Fiber laser," *Nano Res.*, vol. 8, no. 5, pp. 1522–1534, 2010.
- [18] M. Z. Hasan and C. L. Kane, "Colloquium: Topological insulators," *Rev. Mod. Phys.*, vol. 82, no. 4, p. 3045, 2010.
- [19] A. B. Khanikaev *et al.*, "Photonic topological insulators," *Nature Mater.*, vol. 12, no. 3, pp. 233–239, 2013.
- [20] F. Bonaccorso and Z. Sun, "Solution processing of graphene, topological insulators and other 2d crystals for ultra-fast photonics," *Opt. Mater. Exp.*, vol. 4, no. 1, pp. 63–78, 2014.
- [21] Y. Huang *et al.*, "Widely-tunable, passively Q-switched erbium-doped fiber laser with few-layer MoS<sub>2</sub> saturable absorber," *Opt. Exp.*, vol. 22, no. 21, pp. 25258–25266, 2014.
- [22] F. Jia, H. Chen, P. Liu, Y. Huang, and Z. Luo, "Nanosecond-pulsed, dual-wavelength passively Q-switched c-cut Nd: YVO laser using a few-layer Bi<sub>2</sub>Se<sub>3</sub> saturable absorber," *IEEE J. Sel. Topics Quantum Electron.*, vol. 21, no. 1, pp. 369–374, Jan./Feb. 2015.
- [23] Z. Luo *et al.*, "Topological-insulator passively Q-switched double-clad fiber laser at 2  $\mu$ m wavelength," *IEEE J. Sel. Topics Quantum Electron.*, vol. 20, no. 5, pp. 1–8, Sep./Oct. 2014.
- [24] H. Elim, W. Ji, A. Yuwono, J. Xue, and J. Wang, "Ultrafast optical nonlinearity in PMMA-TiO<sub>2</sub> nanocomposites," *Appl. Phys. Lett.*, vol. 82, pp. 2691–2693, 2003. DOI: 10.1063/1.1568544.
- [25] K. Iliopoulos *et al.*, "Nonlinear optical response of titanium oxide nanostructured thin films," *Thin Solid Films*, vol. 518, no. 4, pp. 1174–1176, Dec. 2009.
- [26] H. Long, A. Chen, G. Yang, Y. Li, and P. Lu, "Third-order optical nonlinearities in anatase and rutile TiO<sub>2</sub> thin films," *Thin Solid Films*, vol. 517, no. 19, pp. 5601–5604, Aug. 2009.
- [27] H. Long, G. Yang, A. Chen, Y. Li, and P. Lu, "Femtosecond Z-scan measurement of third-order optical nonlinearities in anatase TiO<sub>2</sub> thin films," *Opt. Commun.*, vol. 282, no. 9, pp. 1815–1818, May 2009.

- [28] F. Moslehirad, M. H. M. Ara, M. J. Torkamany, and J. Sabbaghzadeh, "Nonlinear optical response of Titania nanoparticles prepared by pulsed laser ablation," *Phys. Procedia*, vol. 19, pp. 152–157, 2011.
- [29] B. Karunakaran, K. Kim, D. Mangalaraj, J. Yi, and S. Velumani, "Structural, optical and Raman scattering studies on DC magnetron sputtered titanium dioxide thin films," *Sol. Energy Mater. Sol. Cells*, vol. 88, no. 2, pp. 199–208, Jul. 2005.
- [30] T. Nambara, K. Yoshida, L. Miao, S. Tanemura, and N. Tanaka, "Preparation of strain-included rutile titanium oxide thin films and influence of the strain upon optical properties," *Thin Solid Films*, vol. 515, no. 5, pp. 3096–3101, Jan. 2007.
- [31] K. M. Reddy, S. V. Manorama, and A. R. Reddy, "Bandgap studies on anatase titanium dioxide nanoparticles," *Mater. Chem. Phys.*, vol. 78, no. 1, pp. 239–245, Feb. 2003.
- [32] "Titanium dioxide (anatase)," Nat. Inst. Standards Technol. (NIST), Gaithersburg, MD, USA, 2015. [Online]. Available: <http://webbook.nist.gov/cgi/cbook.cgi?ID=C13463677&Type=IR-SPEC&Index=0> - Refs
- [33] N. Satoh, T. Nakashima, K. Kamikura, and K. Yamamoto, "Quantum size effect in TiO<sub>2</sub> nanoparticles prepared by finely controlled metal assembly on dendrimer templates," *Nature Nanotechnol.*, vol. 3, no. 2, pp. 106–111, 2008.
- [34] E. Garmire, "Resonant optical nonlinearities in semiconductors," *IEEE J. Sel. Topics Quantum Electron.*, vol. 6, no. 6, pp. 1094–1110, Nov./Dec. 2000.
- [35] Y. Chen *et al.*, "Large energy, wavelength widely tunable, topological insulator Q-switched erbium-doped fiber laser," *IEEE J. Sel. Topics Quantum Electron.*, vol. 20, no. 5, pp. 315–322, Sep./Oct. 2014.
- [36] H. Li *et al.*, "Passively Q-switched erbium-doped fiber laser based on few-layer MoS<sub>2</sub> saturable absorber," *IEEE Photon. Technol. Lett.*, vol. 27, no. 1, pp. 1041–1135, Jan. 2015.
- [37] T. Jiang *et al.*, "Passively Q-switching induced by gold nanocrystals," *Appl. Phys. Lett.*, vol. 101, no. 15, 2012, Art. ID 151122.
- [38] I. S. Moskalev *et al.*, "Highly efficient, narrow-linewidth, and single-frequency actively and passively Q-switched fiber-bulk hybrid Er: YAG lasers operating at 1645 nm," *Opt. Exp.*, vol. 16, no. 24, pp. 19427–19433, 2008.
- [39] R. I. Woodward *et al.*, "Wideband saturable absorption in few-layer molybdenum diselenide (MoSe<sub>2</sub>) for Q-switching Yb-, Er- and Tm-doped fiber lasers," *Opt. Exp.*, vol. 20, no. 15, 2015, Art. ID 237038.
- [40] Y. Chen *et al.*, "Mechanically exfoliated black phosphorus as a new saturable absorber for both Q-switching and mode-locking laser operation," *Opt. Exp.*, vol. 23, no. 10, pp. 12823–12833, 2015.